

Major Project Report on

MEDICAL IMAGE SEMANTIC SEGMENTATION

Megh Manoj Bhalerao (166100-16EE234)

Under the Guidance of,

Dr. Krishnan CMC

Department of Electrical and Electronics Engineering, NITK Surathkal

Date of Submission: 11-28-2019

in partial fulfillment for the award of the degree

of

Bachelor of Technology

In

Electrical and Electronics Engineering

At



Department of Electrical and Electronics Engineering
National Institute of Technology Karnataka, Surathkal

NATIONAL INSTITUTE OF TECHNOLOGY KARNATAKA

Department of Electrical and Electronics Engineering



CERTIFICATE

This is certify that the thesis entitled **Medical Image Semantic Segmentation**, submitted by **Megh Manoj Bhalerao (166100-16EE234)** is a record of bonafide work carried out by them, in the partial fulfilment of the requirement for the award of Degree of B.Tech in Electrical and Electronics Engineering at National Institute of Technology Karnataka, Surathkal.

Dr. Krishnan CMC

Assistant Professor
Department of EEE
NITK, Surathkal

ACKNOWLEDGEMENT

I would like to thank Dr. Spyridon Bakas, Center for Biomedical Image Computing and Analytics (CBICA), University of Pennsylvania, for providing me with this six-month internship opportunity and being a great mentor. I would like to thank all the members of the Section of Biomedical Image Analysis (SBIA) for their help and support. I would like to thank Professor Krishnan CMC for being my internal project supervisor without whose support it would not been possible to conduct the project. Last but not the least, I would like to thank my parents and friends for their encouragement and support to pursue this internship.

Abstract

We propose a deep learning based approach for automatic brain tumor segmentation utilizing a three-dimensional U-Net extended by residual connections. In this work, we did not incorporate architectural modifications to the existing 3D U-Net, but rather evaluated different training strategies for potential improvement of performance. Our model was trained on the dataset of the International Brain Tumor Segmentation (BraTS) challenge 2019 that comprise multi-parametric magnetic resonance imaging (mpMRI) scans from 335 patients diagnosed with a glial tumor. Furthermore, our model was evaluated on the BraTS 2019 independent validation data that consisted of another 125 brain tumor mpMRI scans. The current results that our 3D Residual U-Net obtained on the BraTS 2019 validation data are *Dice* scores of 0.6667, 0.85269, 0.70912 and *Hausdorff*₉₅ distances of 7.27002, 8.07931, 9.57081 for enhancing tumor, whole tumor, and tumor core, respectively.

Keywords: *Semantic Segmentation, Brain Tumor Segmentation, Deep Learning, CNN, Glioblastoma, Segmentation, BraTS*

Contents

1	Introduction	1
2	Materials and Methods	2
2.1	Data	2
2.2	Data Pre-processing	3
2.3	Network Architecture	3
2.4	Training Procedure and Hyper-parameters	4
3	Results	7
4	Discussion	7
4.1	Modality Modification	7
4.2	Post-Processing	7
4.3	Modification of loss functions	8
4.4	Architectural Modifications	8

List of Figures

2.1	An example of 4 mpMRI scans with the corresponding label map, comprising the tumor sub-structures.	2
2.2	The architecture followed by our model.	3

1 Introduction

Gliomas are the most common type of adult brain tumors arising from glial cells. They are classified into High Grade Glioma (HGG - also referred to as Glioblastoma) and Lower Grade Glioma (LGG). Patients diagnosed with an LGG have better prognosis than an HGG patient. Multi-parametric Magnetic Resonance Imaging (mpMRI) is generally used by radiologists to detect the tumorous region in the brain to plan treatment and surgery, as well as post-operative monitoring of the patient.

The shape and structure of gliomas are highly variable making their detection and classification a tedious task, hence making the need for automatic segmentation algorithms imminent. Several machine learning approaches have been propounded in the past, with the most recent advent of deep learning (i.e., Convolutional Neural Networks) showing state-of-the-art performance in several segmentation tasks [1, 2, 3, 4, 5]. The crux of segmentation tasks lies in being able to extract global context as well as local information, which is effectively done by the encoder-decoder architecture of the 3D Residual U-net.

2 Materials and Methods

2.1 Data

To create our model we used the publicly available training dataset of the International Brain Tumor Segmentation (BraTS) challenge 2019 comprising mpMRI scans of 259 HGG and 76 LGG subjects (335 in total) [6, 7, 8, 9, 10]. For every subject, there are four available co-registered and skull-stripped mpMRI modalities, namely native T1-weighted (T1), post-contrast T1-weighted (T1CE/T1Gd), T2-weighted (T2), and T2 Fluid Attenuated Inversion Recovery (FLAIR). Every subject was also accompanied by a corresponding ground-truth tumor segmentation label map. These label maps are manually-annotated by expert radiologists. The isometric view of the modalities along with the segmentation label is illustrated below.

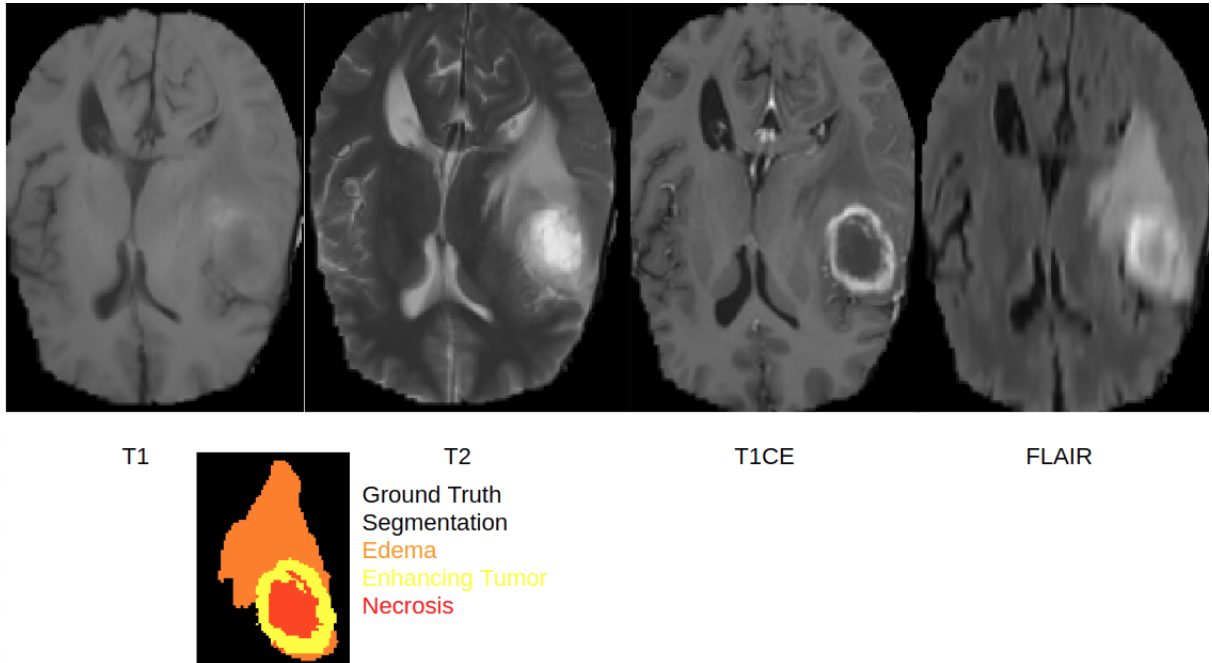


Figure 2.1: An example of 4 mpMRI scans with the corresponding label map, comprising the tumor sub-structures.

Specifically, the tumor label map is divided into 3 regions; non-enhancing tumor core and necrosis (label 1), enhancing tumor core (label 4), and peritumoral edema (label 2), as shown in Fig.2.1. The performance metrics used for the segmentation algorithms are the Dice score, the 95 percentile of the Hausdorff Distance, as well as Sensitivity and Specificity.

2.2 Data Pre-processing

The original MRI scans have lots of background voxels with zero intensity value. For computational efficiency we focus on a region of interest (RoI), *i.e.*, the brain. To achieve this, we obtain a bounding box for all non-zero values across all four mpMRI modalities, and crop each of them according to the largest bounding box (amongst the four modalities), to accommodate the Brain-Region in all the four modalities.

After the bounding-box cropping of all mpMRI scans, we pad the images with zeros along every dimension, with the number of zeros chosen such that to make every dimension divisible by 16, and hence account for 4 downsampling layers in our U-Net architecture. We further normalize each image by $\frac{x-\mu}{\sigma}$, where μ and σ are the mean and standard deviation of that particular image’s intensity values (it must be noted here that the normalization is done by calculating the μ & σ values only of the non-zero regions of the image). Furthermore, we apply N3 bias field correction to the BraTS data.

2.3 Network Architecture

We use the 3D U-Net from [11, 12] with skip/residual connections as illustrated in Fig.2.2.

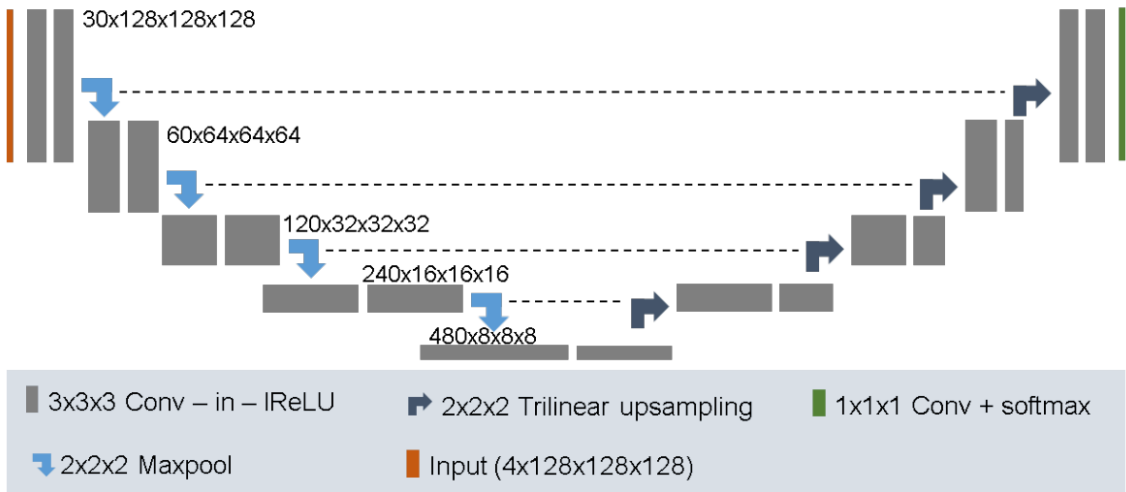


Figure 2.2: The architecture followed by our model.

Our proposed U-Net network is a fully convolutional architecture, meaning that the input image size to the network does not need to be constant (until it meets a certain criteria). The U-Net is an encoder-decoder architecture with 4 downsampling and upsampling modules. The encoder section of the network deciphers semantic information by down-sampling operations, but at the same time loses spatial information due to reduction of image size. This lost spatial information is recovered by the upsampling layers, which perform upsampling using transpose-convolution. A non-linear activation function - Leaky Rectified Linear Unit (leaky ReLU) [13] is applied before every convolution layer, with a leakiness of 10^{-2} . Also since Instance Normalization [14] has been shown to give better results for Image Related Tasks we use Instance Norm instead of Batch-Normalization. In order to avoid the computational bottleneck at the bottom of the "U", skip connections are used which simply concatenate the feature maps of the corresponding upsampling & downsampling layers, so enough contextual information is provided to the network.

Every convolutional module comprises of 2 convolutional layers with the following pipeline : Input \rightarrow Instance Norm \rightarrow Leaky ReLU \rightarrow Convolution \rightarrow Dropout \rightarrow Instance Norm \rightarrow Leaky ReLU \rightarrow Convolution \rightarrow Output (+Input). As we see, we add the input to the output (residual connection), to give something as a shape prior.

At the beginning of the network we start off with 30 filters, successively doubling it with every down-sampling module, reaching a maximum of 480 filters at the bottom of the U. To reduce the computational requirement the number of feature maps is reduced to half, just before the first upsampling layer.

2.4 Training Procedure and Hyper-parameters

Feeding the entire 3D mpMRI scan to the network is very computationally expensive, requiring more than 12 GB of GPU memory, hence we experiment with different divisible-by-16 patch sizes and choose the largest one that fits in the memory. We use a batch-size of 1, again due to com-

putational limitations. The largest image patch that can be employed given computational limitations we want to impose (i.e., 12 GB GPU) is $(128 \times 128 \times 128)$. Randomly extracted patches are used to feed our network. 50 Images are randomly taken from the entire training dataset and are used for internal validation of the model during each epoch. Furthermore, we keep a track of which epoch gives us the best validation loss, and that epoch’s model is used to generate the segmentations on the actual validation data. We start with a learning rate of 0.001, using a triangular schedule, with the minimum learning rate being 0.000001. Our learning rate varies in a triangular wave like fashion between these two maximum and minimum values, being updated after every iteration (*i.e.*, after every forward pass + back-propagation). This learning rate schedule is used to avoid the local minima spots where the weights might get stuck if we use a monotonically decreasing learning rate. The model is trained for 100 epochs with no-early stopping being done as of now. A stochastic gradient optimizer is used with a momentum of 0.9.

Our model segments the input into the 3 BraTS classes as mentioned above (in addition to 1 background class since we use a soft-max activation in the final layer). Since the most important metric used to quantitatively evaluate the segmentation performance is the Dice score, we continuously optimize towards maximizing the Dice. In the problem statement of BraTS there is an issue of class imbalance (i.e., the background/brain pixels are a lot more in number than the pixels of the segmentation labels). To partially tackle this issue of class imbalance, the Multi-Class dice loss function is used here. This calculates the Dice for individual classes and then averages them. The multi-class dice loss function used is as follows:

$$\ell_{mcd} = 1 - \frac{2}{K} \sum_K \frac{\sum_i u_i^k v_i^k}{\sum_i u_i^k + \sum_i v_i^k} \quad (1)$$

where K is the number of classes, k is the k^{th} class, and i is the i^{th} pixel, u is the predicted soft-max probability for the k^{th} class, and v is the one hot encoded ground truth of the corresponding k^{th} class.

Since medical image datasets are generally smaller compared to other semantic segmentation tasks and the U-Net is a fairly deep network, there arises the issue of overfitting. This is tackled by data augmentation techniques - as of now we are using 90-degree rotation, mirroring, and 45-degree rotation. Furthermore, we add Gaussian noise to every training image, with a $\mu = 0$ and a $\sigma = 0.1$ so as to improve the generalization ability of the network on unseen data.

3 Results

We generate the predicted segmentation labels by thresholding our output probability map for the 125 validation cases with 0.5 as the threshold. The results on the validation are shown below:

Table 1: Results on BraTS 2019 Validation Data

	Dice			Haus		
	Enh.	Whole.	Core.	Enh.	Whole.	Core.
Mean	0.66677	0.85269	0.70912	7.27002	8.07931	9.57081
Std. Dev	0.29306	0.15486	0.27646	12.50261	13.56434	12.50147
Median	0.77811	0.90147	0.82969	2.44949	3.60555	4.89898

4 Discussion

Our model has the potential to provide better results with further improvements in our training process. Below we are listing some of the modifications which we are going to make to the existing process for improvement performance, before the BraTS 2019 testing phase.

4.1 Modality Modification

Presently the four mpMRI scans are being used as is, without any major modifications. We plan to try approaches of adding or substituting an artificially-generated modality, which would give us more meaningful information about the tumor. For example, we plan to run experiments with substituting the T1 and the T2 modality with a thresholded FLAIR image which will give us information about the whole tumor region, which should further improve our performance in this region.

4.2 Post-Processing

We further plan to use Isensee et al.’s post-processing technique to improve the dice score of the enhancing tumor. It is known that LGG patients may have no enhancing tumor at all, hence even a single false-positive voxel prediction would make the ET dice score of that patient 0. To overcome this predicament we calculate an experiment-specific voxel threshold for

enhancing tumor region. If the number of enhancing tumor voxels are less than this threshold we set all of them as necrosis, and if not, we leave it as it is. This threshold is calculated by mean-dice optimization over the BraTS 2019 training data.

4.3 Modification of loss functions

Though the Dice loss is an excellent metric to measure performance and for optimization purposes, it penalizes the False Positive and False Negative terms equally, but in reality, for medical image segmentation, a false negative term is much more dangerous than a false positive term since it means that the disease has not been detected at a place where it should have been. This issue can be addressed by using the Tversky Loss Function [15], which penalizes the false negative terms more than the false positive ones, and therefore improves performance. The mathematical expression for the Tversky Loss is given below:

$$\ell_{tv} = 1 - \frac{1}{K} \sum_K \frac{\sum_i u_i^k v_i^k}{\alpha \sum_i u_i^k + \beta \sum_i v_i^k} \quad (2)$$

All the terms are the same as Multi-class dice loss, except the additional parameters α and β , where $\alpha + \beta = 1$, and $\beta > 1$. The $\beta > 1$ ensures that the FN terms are penalized more than the FP ones. The Multi-class dice loss is a special case of the Tversky loss where $\alpha = \beta = 0.5$. Also, cross entropy loss could be used in conjunction with either the dice loss or the Tversky loss.

4.4 Architectural Modifications

Architectural modifications such as incorporation of inception modules instead of simple convolutional layers have the potential to improve the performance. Inception modules perform convolutions in-parallel with different filter sizes on the input feature map. Paralleled convolutions also help in reduction of bottle-necking of features as compared to convolutions performed sequentially, since multi-scale features can be detected by different filter sizes. The outputs of these parallel paths are then "depth"-concatenated.

References

- [1] K. Kamnitsas, C. Ledig, V. F. Newcombe, J. P. Simpson, A. D. Kane, D. K. Menon, D. Rueckert, and B. Glocker, “Efficient multi-scale 3D CNN with fully connected CRF for accurate brain lesion segmentation,” *MIA*, vol. 36, pp. 61–78, 2017.
- [2] F. Isensee, P. Kickingereder, W. Wick, M. Bendszus, and K. H. Maier-Hein, “Brain tumor segmentation and radiomics survival prediction: Contribution to the brats 2017 challenge,” in *International MICCAI Brainlesion Workshop*. Springer, 2017, pp. 287–297.
- [3] X. Li, H. Chen, X. Qi, Q. Dou, C.-W. Fu, and P. A. Heng, “H-denseunet: Hybrid densely connected unet for liver and liver tumor segmentation from ct volumes,” *arXiv preprint arXiv:1709.07330*, 2017.
- [4] F. Isensee, P. F. Jaeger, P. M. Full, I. Wolf, S. Engelhardt, and K. H. Maier-Hein, “Automatic cardiac disease assessment on cine-mri via time-series segmentation and domain specific features,” in *International Workshop on Statistical Atlases and Computational Models of the Heart*. Springer, 2017, pp. 120–129.
- [5] K. Kamnitsas, W. Bai, E. Ferrante, S. McDonagh, M. Sinclair, N. Pawlowski, M. Rajchl, M. Lee, B. Kainz, D. Rueckert et al., “Ensembles of multiple models and architectures for robust brain tumour segmentation,” in *International MICCAI Brainlesion Workshop*. Springer, 2017, pp. 450–462.
- [6] Bakas, S., et al. ”Advancing the cancer genome atlas glioma MRI collections with expert segmentation labels and radiomic features.” *Nature Scientific Data* 4:170117, 2017.
- [7] Bakas, S., et al. ”Segmentation labels and radiomic features for the pre-operative scans of the TCGA-GBM collection.” *The Cancer Imaging Archive* 286, 2017.
- [8] Bakas, S., et al. ”Segmentation labels and radiomic features for the pre-operative scans of the TCGA-LGG collection.” *The Cancer Imaging Archive*, 2017.

- [9] Menze BH, Jakab A, Bauer S, et al. The Multimodal Brain Tumor Image Segmentation Benchmark (BRATS). *IEEE Trans Med Imaging*. 2015;34(10):1993–2024. doi:10.1109/TMI.2014.2377694
- [10] S. Bakas, M. Reyes, A. Jakab, S. Bauer, M. Rempfler, A. Crimi, et al., "Identifying the Best Machine Learning Algorithms for Brain Tumor Segmentation, Progression Assessment, and Overall Survival Prediction in the BRATS Challenge", *arXiv preprint arXiv:1811.02629* (2018)
- [11] O. Çiçek, A. Abdulkadir, S. S. Lienkamp, T. Brox, and O. Ronneberger, "3d u-net: learning dense volumetric segmentation from sparse annotation," in *International Conference on Medical Image Computing and Computer-Assisted Intervention*. Springer, 2016, pp. 424–432.
- [12] Isensee F., Kickingereder P., Wick W., Bendszus M., Maier-Hein K.H. (2018) Brain Tumor Segmentation and Radiomics Survival Prediction: Contribution to the BRATS 2017 Challenge. In: Crimi A., Bakas S., Kuijf H., Menze B., Reyes M. (eds) *Brainlesion: Glioma, Multiple Sclerosis, Stroke and Traumatic Brain Injuries. BrainLes 2017. Lecture Notes in Computer Science*, vol 10670. Springer, Cham
- [13] Arora, R., Basu, A., Mianjy, P., and Mukherjee, A. (2016). Understanding deep neural networks with rectified linear units. *arXiv preprint arXiv:1611.01491*.
- [14] D. Ulyanov, A. Vedaldi, and V. Lempitsky. Instance normalization: The missing ingredient for fast stylization. *arXiv preprint arXiv:1607.08022*, 2016.
- [15] Salehi S.S.M., Erdogmus D., Gholipour A. (2017) Tversky Loss Function for Image Segmentation Using 3D Fully Convolutional Deep Networks. In: Wang Q., Shi Y., Suk H.I., Suzuki K. (eds) *Machine Learning in Medical Imaging. MLMI 2017. Lecture Notes in Computer Science*, vol 10541. Springer